Effect of Power Factor of a Synchronous Machine on Eccentricity Faults Classification Accuracies

Latifa Yusuf
Electrical and Computer Engineering
University of Victoria
Victoria, Canada
lyusuf@uvic.ca

Ashwin Shejwalkar
Electrical and Electronics Engineering
BITS Pilani, K.K Birla Boa Campus
Goa India
ashwinshejwalkar@gmail.com

Ilamparithi Thirumarai-Chelvan
Electrical and Computer Engineering
University of Victoria
Victoria, Canada
ilampari@uvic.ca

2024 IEEE Canadian Conference on Electrical and Computer Engineering (CCECE) | 979-8-3503-7162-8/24/$31.00 ©2024 IEEE | DOI: 10.1109/CCECE59415.2024.10667158

***Abstract*— The research work studies the effect of changing power factor of a Salient Pole Synchronous Machine (SPSM) on eccentricity fault classification accuracies of machine learning and deep learning models. The SPSM was subjected to static eccentricity (SE) and dynamic eccentricity (DE) with a severity of forty percent. Data was collected at different operating conditions, such as lagging, leading, and unity power factor. The data was used to train an Artificial Neural Network (ANN) and a one-dimensional Convolutional Neural Network (1D CNN) for eccentricity fault classification. Results show that the SPSM's changing power factor significantly affected the classification accuracy of both neural networks.**

Keywords*— Dynamic Eccentricity (DE), Salient Pole Synchronous Machine (SPSM), Static Eccentricity (SE), power factor (pf)

I. INTRODUCTION

One of the many advantages of synchronous machines used in industries is power factor correction. This is because they can alter the power factor and improve the overall system's efficiency into which they are integrated. Depending on the load or excitation conditions, they are operated at unity, leading, or lagging power factors [1]. However, synchronous machines can develop faults, and one major type of fault that occurs is the eccentricity fault. This fault occurs when the rotor and stator centers are not perfectly aligned. It can lead to poor machine operation, vibration, and loss of efficiency, which can be detrimental. Hence, accurate and reliable condition monitoring is of utmost importance. Eccentricity faults have two categories, namely, static eccentricity (SE) and dynamic eccentricity (DE) [2], [3], [4].

The detection and classification of eccentricity faults have been studied and documented extensively. They can be categorized under two broad headings: invasive and non-invasive. Invasive methods are intrusive methods that require the installation of search coils and hall sensors in the machine [2], [4], [5]. Even though intrusive methods can detect rotor eccentricity faults, they have some shortcomings. They require extra cost, and an expert is needed for their installation. There is also the problem of the reliability and durability of these sensors under harsh industrial conditions.

Non-invasive techniques have been gaining popularity in detecting eccentricity faults. Signals such as current, magnetic flux, vibration, and torque sensed outside the motor are commonly used for eccentricity diagnosis. [5] used accelerometers to measure vibration under offline and online methods to detect SE in an Interior Permanent Magnet Synchronous (IPMSM). Motor Current Signal Analysis (MCSA) is the most common non-invasive method used. It uses signal processing techniques to look for fault indicators in the frequency spectrum of the stator currents [6]. [7] used current signature analysis without machine disassembly to detect SE and DE in a salient pole synchronous machine (SPSM). Harmonic components closer to the fundamental frequency were utilized. Signal processing methods have also been incorporated with MCSA for eccentricity detection. Authors in [8] applied the Fast Fourier Transform (FFT) and Discrete Wavelet Transform (DWT) in conjunction with MCSA and motor vibration signature analysis (MVSA). This hybrid method was used to analyze frequency components of the stator current in an induction motor for SE detection. Continuous Wavelet Transform (CWT) was used by the authors in [9] to detect eccentricity by decomposing, analyzing, and identifying faulty indices from the frequency components of the stator of an inverter-fed induction machine. It is safe to mention that MCSA is affected by noise and vibration. It can also be challenging to distinguish the indices and indicators used in identifying eccentricity from other types of faults. Furthermore, there is the issue of load variation, which can introduce unintended harmonics to the current signature of the machine [10], [11], [12].

Recently, Machine Learning (ML) and Deep Learning (DL) have been used to classify, predict, and estimate eccentricity fault severities. They are data-driven and eliminate the need for cumbersome mathematical machine models. In addition, they can effectively be used in both offline and online detection schemes. The most used ML algorithms for eccentricity fault classification and severity estimation are K-Nearest Neighbor (k-NN) [13], Decision Tree (DT) [14], Support Vector Machine (SVM) [15], Random Forest Tree (RFT) and Artificial Neural Network (ANN) [16]. A dimensionality reduction technique called Principal Component Analysis (PCA) has also been recently used to segregate DE from SE in an SPSM at different loading conditions [17].

Faulty and healthy machine data are processed, and features are extracted for ML classification algorithms. On the other hand, DL algorithms do not require manual feature selection. Convolutional Neural Networks (CNN) have been used by researchers to detect bearing faults and broken rotor bar faults,

as reviewed in articles [18], [19]. However, authors in [19] used CNN to differentiate between broken rotor bars and eccentricity faults in an induction machine. The results were compared with the conventional MCSA method and FFT-SVM ML algorithm. CNN proved to be able to extract complex features for accurate classification and severity estimation. [20] also classified between demagnetization and eccentricity faults using an image recognition-based deep CNN in a PMSM. The method used an autocorrelation matrix to define feature representations of the stator currents. An accuracy of 98.7 % was achieved. In [21], a comparative study of ANN and CNN for SE and DE classification was performed. Stator and field currents of an SPSM were used as input into the neural networks, and the performance was compared based on accuracy and computational complexity.

As stated earlier, synchronous machines are mainly used for power factor correction in industries. Using ML and DL, their effect on fault classification has yet to be studied to the best of our knowledge. Hence, it is imperative to study how different power factor operations of a synchronous machine affect ML and DL model accuracies. This work focuses on how changing power factor conditions of an SPSM affects the eccentricity fault classification of SE and DE at different loading conditions. ANN and one-dimensional CNN (1D CNN) models are considered and analyzed using stator currents as input.

II. MODELS USED

The two data-driven models used for this study are described briefly below.

A. *Artificial Neural Network (ANN)*

An ANN's architecture typically features three distinct layers: input, hidden, and output. Mimicking the human brain's structure, ANNs are composed of neurons arranged in a complex, nonlinear network, as shown in Fig. 1[22]. These neurons are interconnected through links that carry weights, establishing a sophisticated web of communication pathways. The operational framework of ANNs encompasses various processes. These include gathering and analyzing data and crafting the network structure. The number of hidden layers, the simulation of the network, and the calibration of weights and biases are also considered. These activities are all guided and refined through dedicated learning and training methodologies.

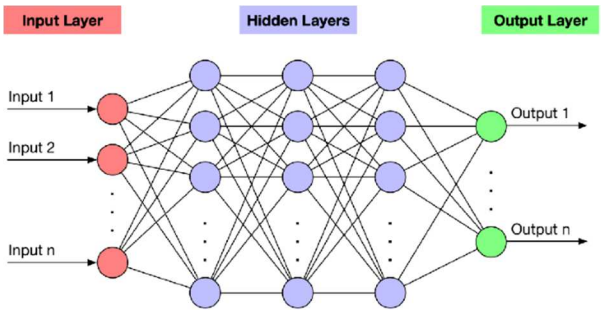

Fig. 1 Artificial Neural Network Architecture [23]

B. *One-Dimensional Convolutional Neural Network (1D CNN)*

Convolutional Neural Networks (CNNs) are a specialized type of feed-forward neural networks characterized by their deep architecture consisting of multiple hidden layers. Unlike the fully connected approach seen in other network types, these networks distinguish themselves by employing convolution operations in their connections. This fundamental difference allows CNNs to learn feature extraction autonomously. Thus, the need for manual feature selection and data preprocessing, typical of traditional classification methods, is eliminated. 1D CNN is characterized by the type of input into the CNN and the sliding features of the filter. For time series input data, the filter moves only in one direction[24]

In the convolution process, kernels are utilized to identify features within localized sections of the input, sliding across it to create maps that signify identified features. Each neuron output within these maps is connected to a distinct portion of the layer before it is termed the receptive field. Multiple kernels within a convolutional layer allow for extracting various features, equating the number of kernels to the output channels. To add complexity to the model, activation functions like rectified linear unit (ReLU) are incorporated after convolution. The pooling technique minimizes the input's dimensionality, aiding in capturing a broader array of features and enhancing the model's adaptability to minor positional changes of features. Finally, the network utilizes these processed features in its final stage, predicting the classification probabilities with a SoftMax function in a densely connected layer, streamlining the model's ability to discern and classify the input efficiently. [24], [25]. A 1D CNN is depicted in Fig. 2.

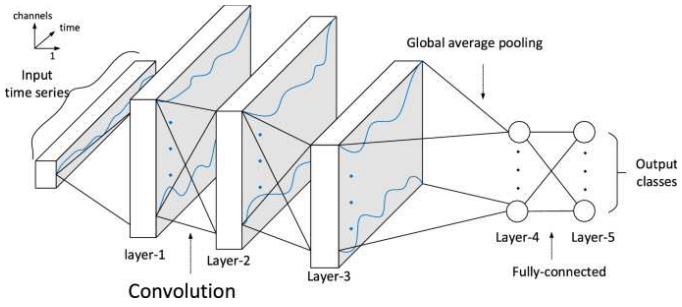

Fig. 2 1D CNN architecture [24]

As the filter traverses the input data, (1) derives the neuron's value in the subsequent layer [26].

$$x^{k+1} = f\left(\sum_{i=1}^{l} w_i . s_i^k + b^k\right) \quad (1)$$

where x is the next layer neuron

k = layer
b^k = bias

w = filter with length l
s = receptive field
f = Activation function

III. EXPERIMENTS

In an experimental setup involving a 3-phase, 2 kW, 4-pole SPSM, modified bushings were used to introduce 40% SE and DE one at a time. By eccentrically cutting bushings and positioning them differently, offsets in the airgap were created. The SE bushings were placed on the end plates, and the DE bushings were placed on the motor shaft. The motor's bearings and end plates were adapted to fit these custom bushings. A 208V, 3-phase voltage, and 60Hz frequency supply from an autotransformer powered the SPSM. To investigate how changes in power factor impact the system, the SPSM was operated under three distinct power factor conditions: 0.9 lagging, 0.9 leading, and unity. These variations were achieved by adjusting the excitation current. For data collection, a Data Acquisition System (DAQ) was employed to record steady-state line currents and line-to-line voltages over 15 seconds at a 3600Hz sampling rate. A high sampling rate ensures an accurate representation of the original signal. For each motor condition (healthy, 40SE, and 40DE), 54000 samples were collected to provide ample data for training. The loading conditions of the SPSM for each fault condition were 25%, 50%, 75%, full load, and no load. The experimental setup is shown in Fig. 3.

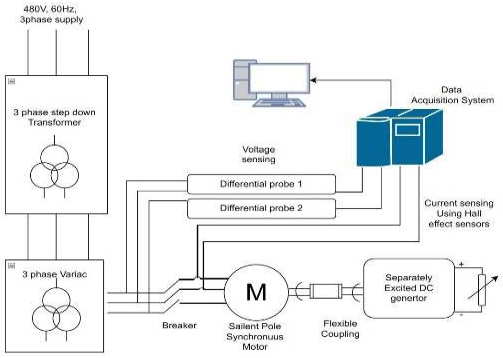

Fig. 3 Experimental setup of SPSM connected to an exciter and DAQ system.

IV. METHODOLOGY

This research aims to study how the power factor of an SPSM affects the ANN and 1D CNN classification of SE and DE. To augment the data, the current data collected from the DAQ is divided into smaller subsets of six complete cycles. The sequence length in each subset was chosen as a multiple of the supply frequency. This is because some of the statistical features used to train the ANN are highly dependent on the periodicity of the input sine wave. Afterward, the current data was rescaled and normalized before training for both neural networks[21]. This is shown in Fig. 4.

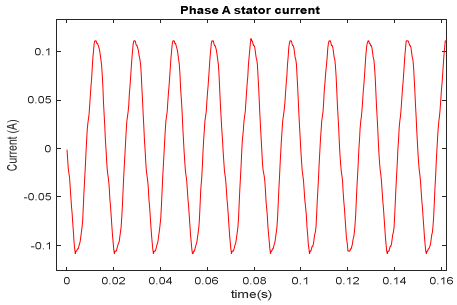

(a)

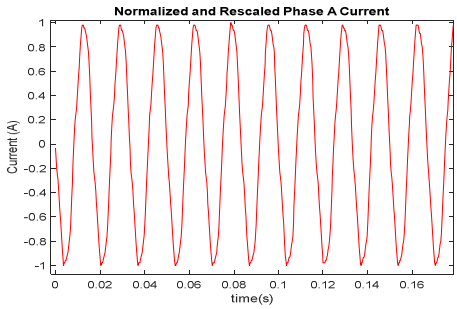

(b)

Fig. 4 (a) Raw stator current (b) Preprocessed stator current

A. Training of ANN

Feature selection is mandatory to train the ANN for eccentricity classification. Statistical features such as mean, root mean square, kurtosis, standard deviation, and skewness were used. They are expressed in (2)-(6), respectively.

$$\mu = \frac{1}{N}\sum_{i=1}^{N} x_i \tag{2}$$

$$RMS = \sqrt{\frac{1}{N}\sum_{i=i}^{N} x_i^2} \tag{3}$$

$$\kappa = \frac{1}{N}\sum_{i=i}^{N} \frac{(x_i - \mu)^4}{\sigma^4} \tag{4}$$

$$\sigma = \sqrt{\frac{1}{N}\sum_{i=i}^{N} (x_i - \mu)^2} \tag{5}$$

$$Sk = \frac{1}{N}\sum_{i=i}^{N} \frac{(x_i - \mu)^2}{\sigma^3} \tag{6}$$

where: x_i is the *ith* observation
N is the number of observations.

Before the ANN's training begins, the configuration settings external to the model must be set. These settings are called the

network's hyperparameters. The hyperparameters for both neural networks were selected through random search and then fine-tuned for better accuracy and training efficiency. Tables I and II summarize the parameters used.

B. Training of 1D CNN

Feature selection is unnecessary for CNN. Hence, the preprocessed stator current is fed directly into the network. The CNN architecture used for training the model comprises an input layer, three convolutional layers, an average pooling layer, one fully connected area, and one classification layer. The classification layer categorizes the data into healthy, SE, or DE. A filter size of 8 was used for all convolutional layers. The number of filters for the first convolutional layer was 16. It was configured to be double as it transverses the second and third convolutional layers. This increases the feature extraction capability to learn complex relationships between the features easily. The Global Average pooling was set for the pooling area for dimensionality reduction. The Rectified Linear Unit (ReLU) function is applied to the output of the pooling area to introduce non-linearity into the model. Since CNNs are easily prone to overfitting, a dropout factor of 0.1 and a lambda value of 0.0001 were initialized in the model. This also helps with the generalization of the testing data. All hyperparameters configured for the network are listed in Table II.

TABLE I. HYPERPARAMETER FOR ANN

Hyperparameter	Value
Layer sizes	50
Activations	Tanh
Layer Weight Initializer	Glorot
Layer Biases Initializer	Zeros
Solver	LBFGS
Output Layer Activation	SoftMax
Lambda	0

TABLE II. HYPERPARAMETER FOR 1D CNN

Hyperparameter	Value
Initial Learning rate	$\mathbf{1 \times 10^{-3}}$
Activation	ReLU
Lambda	$\mathbf{1 \times 10^{-3}}$
Solver	ADAM
Epsilon	$\mathbf{1 \times 10^{-8}}$
Output Layer Activation	SoftMax
Lambda	0.0001

V. RESULTS & DISCUSSION

To analyze the effect of power factor on the classification of SE and DE, the confusion matrix chart was used to see the accuracies of each neural network. To test and achieve this, the following steps were carried out in MATLAB.

A. ANN

Data was collected for three power factor (pf) conditions (unity, 0.9 lagging, and 0.9 leading). The preprocessed data was used as input into the ANN. Four scenarios were considered, as shown in Table III. To test for the accuracy of the model, each scenarios were executed.

TABLE III TRAINING AND TESTING DATA FOR ANN AND 1D CNN

Scenario	Training Data	Testing Data
1	All lagging pf for healthy, 40SE, and 40DE at no load (NL), full load (FL), 25% full (25FL) load, 50% full load (50FL) combined	Training data is split into 70% training and 30% testing.
2	All lagging pf for healthy, 40SE and 40DE at NL, FL, 25FL, 50FL and 75FL data combined	All leading pf for healthy, 40SE, and 40DE at NL, FL, 25FL, 50FL, and 75FL data combined
3	All lagging pf for healthy, 40SE and 40DE at NL, FL,25FL, 50FL and 75FL data combined	All unity pf for healthy, 40SE, and 40DE at NL, FL, 25FL, 50FL, and 75FL data combined
4	All lagging, leading, and unity pf for healthy, 40SE, and 40DE at NL, FL, 25FL, 50FL, and 75FL data combined.	A completely new set of lagging, leading, and unity pf for healthy, 40SE, and 40DE at NL, FL, 25FL, 50FL, and 75FL data combined

a) Scenario 1

As shown in Figure 5, an accuracy of 100% was obtained. This shows that the model can accurately classify SE and DE under lagging conditions.

b) Scenario 2

As shown in Figure 6, an accuracy of 47% was obtained. The predicted values for each motor condition are shown in the confusion matrix. The results below show that the ANN's learned features for the SPSM's lagging conditions have significantly been altered by the leading pf.

c) Scenario 3

Similarly, as shown in Fig. 7, an accuracy of 46.67% was obtained. This is consistent with the previous result in scenario 2. The learned features by the ANN have been altered by unity pf.

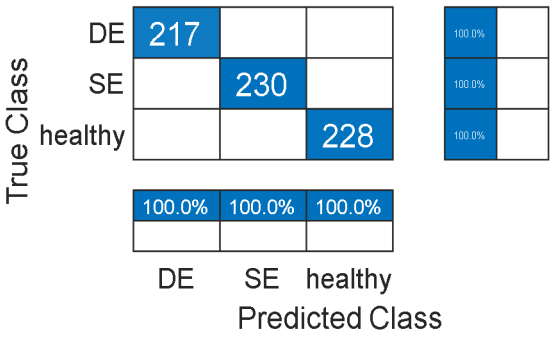

Fig 5. ANN lagging pf

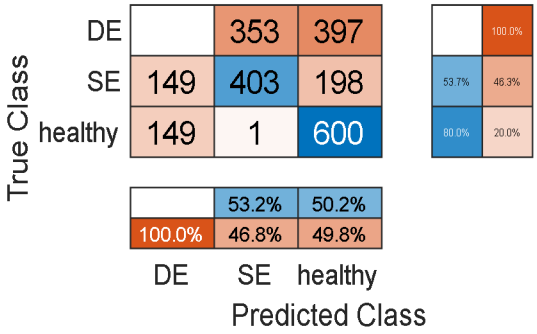

Fig 6. ANN leading pf

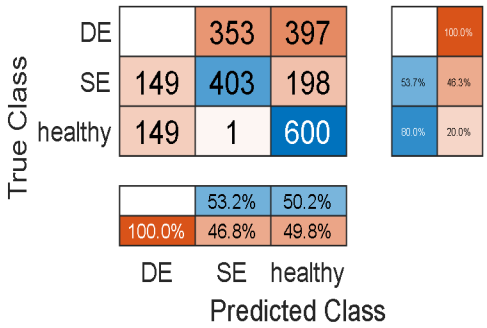

Fig 7. ANN unity pf

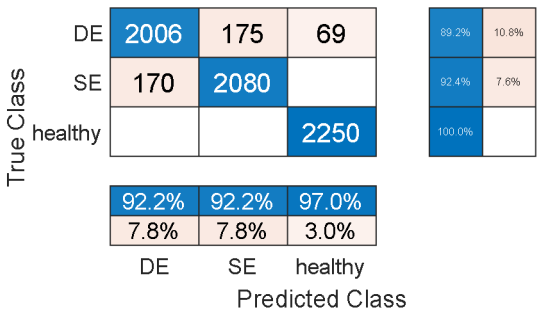

Fig 8. ANN- all pf Combined

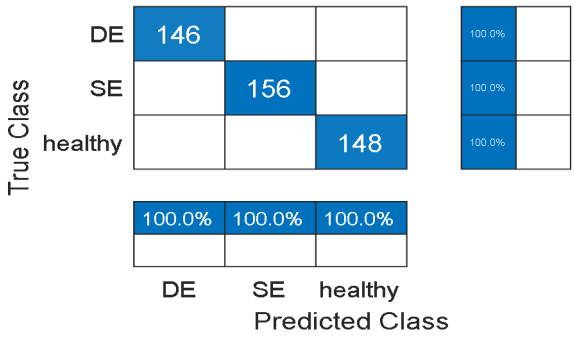

Fig.9 1D CNN-lag pf – 100% accuracy

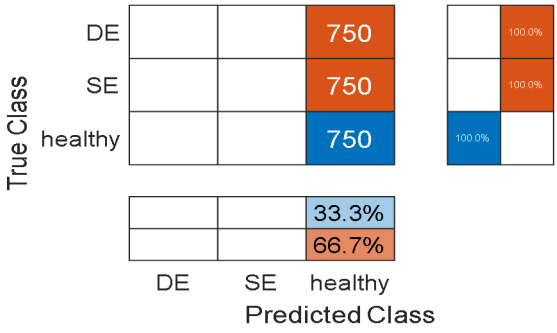

Fig.10 1D CNN-lead pf – 33.3% accuracy

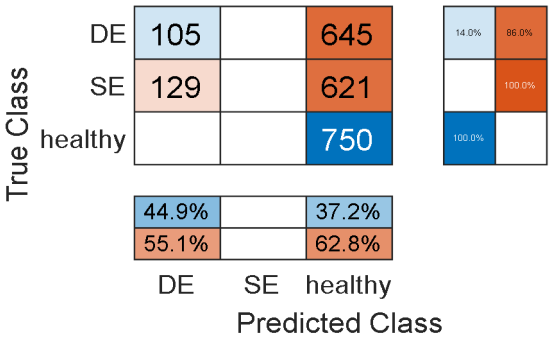

Fig.11 1D CNN-unity pf – 38% accuracy

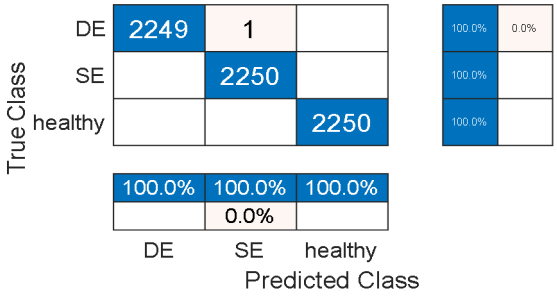

Fig.12 1D CNN-all pf combined- 100% accuracy

d) Scenario 4

An accuracy of 93.87% was obtained, and the confusion matrix is shown in Fig. 8. This shows that the model accuracy improved as all pf cases were used for training the ANN model.

B. 1D CNN

Similarly, the same process, conditions, and scenarios considered for ANN were also used for the 1D CNN. The percentage accuracies and their confusion matrices are depicted in Fig. 9, 10, 11, and 12. The model performed excellently in classifying the SPSM's health condition when trained and tested with the same lagging data. However, when tested with leading and unity pf data, the CNN could not classify SE and DE. In the case of the last scenario, the model performed exceedingly well even though it had not been trained with the testing data before.

VI. CONCLUSION

This work focuses on how an SPSM's changing power factor affects the eccentricity fault prediction accuracies of machine learning and deep learning models. Data was extracted from a healthy and faulty SPSM (40DE and 40 SE) to train an ANN and 1D CNN. Using experimental data captures complex fault dynamics under actual conditions that can be difficult to represent using 3D FEA. Four scenarios were explored, each involving different combinations of training and testing data for each neural network. Both neural networks performed well in classifying SE and DE when the SPSM lagging pf data was used for training and testing. Similarly, they had good accuracy when all the leading, lagging, and unity data was used for training and testing. On the contrary, low accuracies were obtained when the model trained with lagging pf data and was tested with leading or unity pf data. For the ANN, this shows that there is a significant alteration of features learned by the ANN as the power factor of the machine changes. 1D CNN is known to select features automatically by learning intricate patterns from the input data. It suffices to say that its inability to classify SE and DE in the second and third scenarios shows that different pf condition of an SPSM creates patterns and signatures in the stator current data that are unique to each pf condition. For accurate model deployment in real-life applications, it is advisable to use data from the three pf (leading, lagging, and unity) of a synchronous machine for training and accurate classification of eccentricity faults. The scope of the research is focused on synchronous machines [27]; more research is needed to explore other machine learning algorithms, as shown in [28]. Also, future work focusing on the effect of other varying power factors or just a change in the multiplication factor would be explored to test the performance of model accuracies in a synchronous machine.

ACKNOWLEDGMENT

The Natural Sciences and Engineering Research Council of Canada (NSERC) and the Mitacs Globalink Research Internship Program (Mitacs GRI) provided the funding for this research. The University of Victoria provided the necessary research facilities to conduct the research.

REFERENCES

[1] G. Oscarson, I. Jack, and S. Mol, "The ABC's of Synchronous Motors." Accessed: Mar. 05, 2024. [Online]. Available: https://static.weg.net/medias/downloadcenter/hfe/hf4/WEG-the-abcs-of-synchronous-motors-usaem200syn42-brochure-english.pdf

[2] J. H. Im, J. K. Kang, and J. Hur, "Static and Dynamic Eccentricity Faults Diagnosis in PM Synchronous Motor Using Planar Search Coil," *IEEE Transactions on Industrial Electronics*, Sep. 2022, doi: 10.1109/TIE.2022.3212402.

[3] S. Nandi, A. H. Toliyat, and A. H. Toliyat, "Condition Monitoring and Fault Diagnosis of Electrical Machines - A Review," *IEEE Transactions on Industrial Electronics*, 1999, pp. 197–284.

[4] S. Nandi and H. A. Toliyat, "Detection of rotor slot and other eccentricity related harmonics in a three phase induction motor with different rotor cages," *1998 International Conference on Power Electronic Drives and Energy Systems for Industrial Growth, 1998. Proceedings.*, Perth, WA, Australia, 1998, pp. 135-140 Vol.1, doi: 10.1109/PEDES.1998.1330003..

[5] A. Aggarwal and E. G. Strangas, "Review of Detection Methods of Static Eccentricity for Interior Permanent Magnet Synchronous Machine", doi: 10.3390/en12214105.

[6] C. 'Seungdeog, A. T. 'Hamid, N. 'Subhasis, and M. 'Homayoun, *Electric Machines, Modeling, Condition Monitoring and Fault Diagnosis*. Boca Raton, FL, USA: CRC Press, 2013.

[7] T. Ilamparithi, S. Nandi, S. Member, J. Subramanian, and S. Member, "A Disassembly-Free Offline Detection and Condition Monitoring Technique for Eccentricity Faults in Salient-Pole Synchronous Machines," *IEEE Trans Ind Appl*, vol. 51, no. 2, doi: 10.1109/TIA.2014.2358797.

[8] N. Bessous, S. E. Zouzou, S. Sbaa, W. Bentrah, Z. Becer and R. Ajgou, "Static eccentricity fault detection of induction motors using MVSA, MCSA and discrete wavelet transform (DWT)," *2017 5th International Conference on Electrical Engineering - Boumerdes (ICEE-B)*, Boumerdes, Algeria, 2017, pp. 1-10, doi: 10.1109/ICEE-B.2017.8192035.

[9] I. P. Georgakopoulos, E. D. Mitronikas, A. N. Safacas and I. P. Tsoumas, "Detection of eccentricity in inverter-fed induction machines using wavelet analysis of the stator current," *2008 IEEE Power Electronics Specialists Conference*, Rhodes, Greece, 2008, pp. 487-492, doi: 10.1109/PESC.2008.4591976..

[10] R. Supangat, J. Grieger, N. Ertugrul, W. L. Soong, D. A. Gray and C. Hansen, "Investigation of Static Eccentricity Fault Frequencies using Multiple Sensors in Induction Motors and Effects of Loading," *IECON*

2006 - 32nd Annual Conference on IEEE Industrial Electronics, Paris, France, 2006, pp. 958-963, doi: 10.1109/IECON.2006.347647.

[11] R. Alimardani, A. Rahideh, and S. H. Kia, "Mixed Eccentricity Fault Detection for Induction Motors Based on Time Synchronous Averaging of Vibration Signals," 2023, doi: 10.1109/TIE.2023.3266589.

[12] J. Shin, Y. Park, and S. Bin Lee, *Flux-based Detection and Classification of Induction Motor Eccentricity, Rotor Cage, and Load Defects*.

[13] K. Sri Kashyap and P. N. Kumar, "Application of Machine Learning for Analysis of Static Eccentricity Fault in IPMSM using Finite Element Method," *2021 National Power Electronics Conference (NPEC)*, 2021, doi: 10.1109/NPEC52100.2021.9672469.

[14] E. Irgat, A. Ünsal and H. T. Canseven, "Detection of Eccentricity Faults of Induction Motors Based on Decision Trees," *2021 13th International Conference on Electrical and Electronics Engineering (ELECO)*, Bursa, Turkey, 2021, pp. 435-439, doi: 10.23919/ELECO54474.2021.9677809

[15] Y. Yinquan *et al.*, "Rotor Faults Diagnosis in PMSMs Based on Branch Current Analysis and Machine Learning," *Actuators*, vol. 12, no. 4, pp. 1–19, 2023, doi: 10.1109/CIEEC58067.2023.10166472.

[16] I. M. Hussein and Z. Al-Hamouz, "Neural Network Based Detection Technique for Eccentricity Fault in LSPMS Motors," *Proceedings - 2018 Innovations in Intelligent Systems and Applications Conference, ASYU 2018*, pp. 1–5, 2018, doi: 10.1109/ASYU.2018.8554007.

[17] L. Yusuf and T. Ilamparithi, "Dynamic Eccentricity Fault Detection in Synchronous Machines Using Principal Component Analysis," *Canadian Conference on Electrical and Computer Engineering*, vol. 2023-Septe, pp. 348–353, 2023, doi: 10.1109/CCECE58730.2023.10288802.

[18] S. Zhou, L. Lin, C. Chen, W. Pan, and X. Lou, "Application of Convolutional Neural Network in Motor Bearing Fault Diagnosis," 2022, doi: 10.1155/2022/9231305.

[19] F. Dişli, M. Gedikpınar, and A. Sengur, "Deep Transfer Learning-Based Broken Rotor Fault Diagnosis For Induction Motors", *Turkish Journal of Science and Technology*, vol. 18, no. 1, pp. 275–290, 2023, doi: 10.55525/tjst.1261887.

[20] Z. Li, Q. Wu, S. Yang, and X. Chen, "Diagnosis of rotor demagnetization and eccentricity faults for IPMSM based on deep CNN and image recognition," *Complex and Intelligent Systems*, vol. 8, no. 6, pp. 5469–5488, Dec. 2022, doi: 10.1007/s40747-022-00764-z.

[21] A. Shejwalkar, L. Yusuf and T. C. Ilamparithi, "Comparative Analysis of Machine Learning Algorithms for Eccentricity Fault Classification in Salient Pole Synchronous Machine," *2024 IEEE Texas Power and Energy Conference (TPEC)*, College Station, TX, USA, 2024, pp. 1-6, doi: 10.1109/TPEC60005.2024.10472206.

[22] E. Ananias, P. D. Gaspar, V. N. G. J. Soares, and J. M. L. P. Caldeira, "Artificial intelligence decision support system based on artificial neural networks to predict the commercialization time by the evolution of peach quality," *Electronics (Switzerland)*, vol. 10, no. 19, Oct. 2021, doi: 10.3390/electronics10192394.

[23] A. Malekian and N. Chitsaz, "Concepts, procedures, and applications of artificial neural network models in streamflow forecasting," in *Advances in Streamflow Forecasting*, Elsevier, 2021, pp. 115–147. doi: 10.1016/B978-0-12-820673-7.00003-2.

[24] H. I. Fawaz, · Germain Forestier, J. Weber, · Lhassane Idoumghar, and P.-A. Muller, "Deep learning for time series classification: a review," *Data Min Knowl Discov*, vol. 33, pp. 917–963, 2019, doi: 10.1007/s10618-019-00619-1.

[25] Y. Lecun and Y. Bengio, "Convolutional Networks for Images, Speech, and Time-Series," M. A. Airbib., The handbook of brain theory and neural networks MIT Press, 1995.

[26] S. Kiranyaz, O. Avci, O. Abdeljaber, T. Ince, M. Gabbouj, and D. J. Inman, "1D convolutional neural networks and applications: A survey," *Mech Syst Signal Process*, vol. 151, Apr. 2021, doi: 10.1016/j.ymssp.2020.107398.

[27] M. Tajdinian, R. Shirali, B. Behdani, H. Samet and H. R. Chamorro, "An Enhanced Dynamic Phasor Estimation Algorithm for Considering the Behaviour of Distributed Generators in Fault Condition," *2022 IEEE International Conference on Environment and Electrical Engineering and 2022 IEEE Industrial and Commercial Power Systems Europe (EEEIC / I&CPS Europe)*, Prague, Czech Republic, 2022, pp. 1-6, doi: 10.1109/EEEIC/ICPSEurope54979.2022.9854679

[28] S. Afrasiabi, B. Behdani, M. Afrasiabi, M. Mohammadi, Y. Liu and M. Gheisari, "A Comparative Analysis of Artificial Intelligence for Power Transformer Differential Protection," *2021 IEEE International Conference on Environment and Electrical Engineering and 2021 IEEE Industrial and Commercial Power Systems Europe (EEEIC / I&CPS Europe)*, Bari, Italy, 2021, pp. 1-6, doi: 10.1109/EEEIC/ICPSEurope51590.2021.9611033